



HAL
open science

Crystallization of $\text{Ge}_2\text{Sb}_2\text{Te}_5$ nanometric phase change material clusters made by gas-phase condensation

G. Ghezzi, Robert Morel, A. Brenac, Nathalie Boudet, M. Audier, F. Fillot, S. Maîtrejean, Françoise Hippert

► **To cite this version:**

G. Ghezzi, Robert Morel, A. Brenac, Nathalie Boudet, M. Audier, et al.. Crystallization of $\text{Ge}_2\text{Sb}_2\text{Te}_5$ nanometric phase change material clusters made by gas-phase condensation. Applied Physics Letters, 2012, 101, pp.233113. 10.1063/1.4769435 . hal-00989954

HAL Id: hal-00989954

<https://hal.science/hal-00989954>

Submitted on 12 May 2014

HAL is a multi-disciplinary open access archive for the deposit and dissemination of scientific research documents, whether they are published or not. The documents may come from teaching and research institutions in France or abroad, or from public or private research centers.

L'archive ouverte pluridisciplinaire **HAL**, est destinée au dépôt et à la diffusion de documents scientifiques de niveau recherche, publiés ou non, émanant des établissements d'enseignement et de recherche français ou étrangers, des laboratoires publics ou privés.

Crystallization of Ge₂Sb₂Te₅ nanometric phase change material clusters made by gas-phase condensation

G. E. Ghezzi, R. Morel, A. Brenac, N. Boudet, M. Audier, F. Fillot, S. Maitrejean, and F. Hippert

Citation: [Applied Physics Letters](#) **101**, 233113 (2012); doi: 10.1063/1.4769435

View online: <http://dx.doi.org/10.1063/1.4769435>

View Table of Contents: <http://scitation.aip.org/content/aip/journal/apl/101/23?ver=pdfcov>

Published by the [AIP Publishing](#)

Articles you may be interested in

[Nanoscale nuclei in phase change materials: Origin of different crystallization mechanisms of Ge₂Sb₂Te₅ and AgInSbTe](#)

J. Appl. Phys. **115**, 063506 (2014); 10.1063/1.4865295

[Phase change behaviors of Zn-doped Ge₂Sb₂Te₅ films](#)

Appl. Phys. Lett. **101**, 051906 (2012); 10.1063/1.4742144

[Ge₂Sb₂Te₅ phase-change films on polyimide substrates by pulsed laser deposition](#)

Appl. Phys. Lett. **101**, 031905 (2012); 10.1063/1.4737410

[Observation and modeling of polycrystalline grain formation in Ge₂Sb₂Te₅](#)

J. Appl. Phys. **111**, 104308 (2012); 10.1063/1.4718574

[Multi-level phase change memory devices with Ge₂Sb₂Te₅ layers separated by a thermal insulating Ta₂O₅ barrier layer](#)

J. Appl. Phys. **110**, 124517 (2011); 10.1063/1.3672448

The advertisement features a row of several tablet devices displaying the journal's cover. The cover art shows a colorful, swirling pattern. The journal title 'Computing' is at the top, with 'SCIENCE & ENGINEERING' below it. At the bottom of the cover, the text 'MULTISCALE PREDICTION' is visible. In the bottom right corner of the advertisement, the journal's logo 'computing SCIENCE & ENGINEERING' is shown. Below the logo, the text 'AIP'S JOURNAL OF COMPUTATIONAL TOOLS AND METHODS. AVAILABLE AT MOST LIBRARIES.' is written in a large, white, sans-serif font against a dark background.

Crystallization of $\text{Ge}_2\text{Sb}_2\text{Te}_5$ nanometric phase change material clusters made by gas-phase condensation

G. E. Ghezzi,^{1,2} R. Morel,³ A. Brenac,³ N. Boudet,⁴ M. Audier,² F. Fillot,¹ S. Maitrejean,¹ and F. Hippert^{2,5}

¹CEA Leti, Minattec campus, 17 Rue des Martyrs, 38054 Grenoble, France

²LMGP (CNRS, Grenoble INP-Minattec), 3 parvis Louis Néel, 38016 Grenoble, France

³INAC/SP2M and Université Joseph Fourier, CEA Grenoble, 38054 Grenoble, France

⁴Institut Néel, CNRS-UJF, 25 rue des Martyrs, BP 166, 38042 Grenoble, France

⁵LNCMI (CNRS-UJF-UPS-INSA), 25 rue des Martyrs, BP 166, 38042 Grenoble, France

(Received 18 July 2012; accepted 15 November 2012; published online 6 December 2012)

The crystallization behavior of $\text{Ge}_2\text{Sb}_2\text{Te}_5$ nanometric clusters was studied using X-ray diffraction with *in situ* annealing. Clusters were made using a sputtering gas-phase condensation source, which allowed for the growth of well-defined, contaminant-free, and isolated clusters. The average size for the clusters is 5.7 ± 1 nm. As-deposited amorphous clusters crystallize in the fcc cubic phase at 180°C , while for thin films, the phase change temperature is 155°C . This observation illustrates the scalability of the $\text{Ge}_2\text{Sb}_2\text{Te}_5$ phase change from the amorphous to the cubic state in three-dimensionally confined systems in this size range. © 2012 American Institute of Physics. [<http://dx.doi.org/10.1063/1.4769435>]

Phase change materials (PCM) such as $\text{Ge}_2\text{Sb}_2\text{Te}_5$ (GST) display unique properties that allowed for the development of optical storage media, and are also good candidates for application in non-volatile memory (phase change random access memory (PCRAM)).¹ Viable PCRAM applications call for bit volume much smaller than that of optical media and this size reduction opens a number of questions regarding the scalability of PCM, for instance, the size dependence of the crystallization temperature T_x .

In this paper, the use of a sputtering gas-aggregation method for the growth of GST nanometric clusters has allowed the study of the phase transformation in isolated amorphous particles. The crystallization of those clusters is definitely observed and their crystallization temperature is close to that of the bulk material, which is a surprising result for such small particles. The presence of strain in the crystalline clusters has been observed. These two features—low T_x and strain—challenge the assumption that the stress state has a strong impact on the crystallization temperature in low-dimension phase change materials.²

Many studies regarding the scalability of the PCM deal with the thickness dependence of the amorphous to fcc crystalline phase transition in GST thin films.^{2–5} The transition temperature is similar to that of the bulk—close to 155°C —for all films with thicknesses above 10 nm. Below that, the increase in T_x differs from one study to the other: The largest reported value is for 2 nm GST thin films deposited on Si and covered with Al_2O_3 , with $T_x = 380^\circ\text{C}$,³ while only small changes in T_x are measured for GST films sandwiched by ZnS-SiO_2 .^{2,5} These studies illustrate that the cladding material plays a significant role in the thickness dependence of the phase transition.^{2,6} In phase change materials where the phase transition is nucleation-dominated, two mechanisms have been proposed regarding this effect. The first one considers that a strong interface interaction between the PCM and the cladding material impedes the nucleation of crystallites within the layer.⁷ The second one considers a correlation

between the mechanical stress state induced by the cladding material, and the change in T_x .² One difficulty with this approach is that, even in the case where the stress in the cladding layer is known, the evaluation of the level of strain induced in the embedded layer is delicate.⁸ In all cases, due to the 3D confinement, clusters are the ideal system for assessing the size effects that could alter the phase change properties. On one hand, the interface effects are enhanced due to a larger surface/volume ratio and, on the other hand, for isolated clusters in a matrix the plastic relaxation is limited due to the confinement, which can thus affect strain state of the PCM.

Some results with GST nanoclusters have been reported. For nanoclusters made by electron beam lithography with size above 20 nm, no significant change in T_x has been observed⁹ while 15 nm nanoclusters obtained with diblock copolymer transform directly into the hexagonal phase.¹⁰ The growth of GST clusters using laser ablation has been reported, with discrepancies in the reported crystallization behavior.^{11–13} The first results¹¹ indicate that, for 15 nm size-selected clusters, amorphous particles with irregular shape are obtained when the annealing is below 200°C , a mixture of hexagonal and fcc phases is observed when the annealing is above 300°C , whereas the pure fcc phase is observed when annealing is performed above 400°C . A second report indicates clusters with a mixture of amorphous and fcc phase for all temperatures,¹² while a third one indicates mostly amorphous as-prepared particles transforming into a mixture of hexagonal and fcc phases at 100°C , and in a mostly fcc phase at 200°C .¹³ The main conclusion from these studies is that both the cubic fcc and amorphous phases can be observed in nanometric GST clusters. On the other hand, the observation of an unambiguous phase transition from an amorphous to a crystalline structure, at a definite temperature, has not yet been achieved. Moreover, in these studies, the effect of the cladding material on the phase change properties of clusters has not been addressed.

In this paper, we present measurements of the crystallization of GST nanometric clusters with average size 5.7 ± 1 nm, embedded in alumina, and 10 nm GST thin films sandwiched with alumina. Clusters and thin films are prepared in a UHV chamber with a sputtering-gas phase condensation cluster source, which allows for the growth of contaminant-free and isolated ternary particles, and two additional standard sputtering guns for the deposition of GST and alumina thin films.¹⁴ The cluster source consists in a magnetron sputtering head inserted in a liquid nitrogen cooled tube: A $\text{Ge}_2\text{Sb}_2\text{Te}_5$ solid target is DC sputtered in a 0.1 mbar cold argon gas, which makes the sputtered atoms condensate into nanometer-sized clusters as they drift along the gas flow lines in the source. Clusters are expelled through an iris diaphragm in the vacuum, forming a beam which is directed onto the sample in a deposition chamber next to the cluster source. DC magnetron is used for the sputtering of GST thin films (using the same sputtering target as the one used for clusters) and RF magnetron is used for Al_2O_3 . All depositions are made at room temperature. Average cluster size measured with a time of flight mass spectrometer is 5.7 ± 1 nm at half maximum. Clusters morphology was controlled by TEM microscopy: A low density layer of clusters was deposited on copper grids coated with holey carbon films, covered with 1 nm Al_2O_3 . The distribution of clusters on the surface is random. No atomic planes are visible for the clusters and the contrast is similar for all particles, which is an indication that as-deposited clusters are amorphous, as confirmed by X-ray analysis.²³ GST thin films and clusters compositions were measured with Rutherford backscattering spectrometry and particle-induced X-ray emission. Thin films content is Ge:Sb:Te = 23:24:53 (± 3), very close to the $\text{Ge}_2\text{Sb}_2\text{Te}_5 = 22:22:56$ targeted composition, and clusters composition is 28:27:45 (± 3), indicating that the GST clusters are slightly Te depleted, as often reported for GST clusters or thin films,^{3,9,12,15} while the GST sputtered thin films are very close to the nominal $\text{Ge}_2\text{Sb}_2\text{Te}_5$ stoichiometry. Within experimental resolution, the GST clusters composition is identical before and after annealing.

Two types of samples were prepared on Si substrates: The first one consists in 10 nm Al_2O_3 /10 nm GST thin film/10 nm Al_2O_3 , the second one consists in GST clusters multilayer with the following structure: 6 nm Al_2O_3 /(GST clusters layer with 0.07 ML of particles/3 nm Al_2O_3) \times 4/3 nm Al_2O_3 . This later structure—with an average distance between clusters of 15 nm—was chosen to avoid sintering effects during annealing. A 20 nm Al_2O_3 thin film was also grown for background subtraction in the X-ray experiments.

A first set of clusters and thin film samples was annealed under vacuum at 200 °C, hereafter referred to as *ex situ* samples. Temperature was ramped at 10 °C/min, held at 200 °C for 30 min, and ramped down to ambient temperature. X-ray diffraction measurements ($\lambda = 0.69654 \text{ \AA}$) using synchrotron radiation on the BM02 CRG-D2AM beamline (ESRF Grenoble, France) were performed at room temperature on both the *ex situ* and as deposited samples. The spectra were recorded in a reflection geometry with a 4° angle of incidence for the incoming X rays, by means of a 2D CCD detector allowing for a 2θ range between 8° and 26°. For a second set of clusters and thin film samples (*in situ* samples), X-ray diffraction spectra were recorded as a function of the temperature during the annealing, using a domed oven stage. Temperature was increased in 10 °C steps after which spectra were recorded for 26 min. In all cases, the Al_2O_3 blank sample signal, measured in similar conditions, was subtracted to remove the large background from the Si substrate.

The angular integrated intensity from the 2D images²³ is shown in Figure 1. For the as-deposited film, the two broad maxima at $2\theta = 12.9^\circ$ and 21.6° allow to conclude to an amorphous state. Their positions match the first two maxima in the reported GST amorphous structure factor.¹⁶ For the annealed film, Bragg peaks are observed. Their positions can be indexed as a fcc cubic structure. The fcc out of plane lattice parameter¹⁷ is 0.601 ± 0.001 nm that closely matches the lattice parameter reported for bulk GST, $0.60117(5)$ nm.¹⁸ Due to the existence of a texture (see the 2D image in supplementary material), the relative intensity for the peaks is not the one expected for a powder pattern. With as-deposited clusters, the X-ray diffraction spectra show no Bragg peaks. For the 200 °C annealed clusters, one clearly detects the (200) and (220) diffraction Bragg peaks which are the two most intense reflections expected in a powder diffraction pattern from the bulk fcc phase. Indeed, the 2D images are isotropic, indicating the absence of texture in clusters. As expected, due to the smaller crystallite size, the peaks width for the clusters is larger than for the thin film. Besides, a clear shift of the diffraction lines with respect to the bulk position is observed. The fcc out of plane lattice parameter for the crystalline clusters calculated from the (200) and (220) peaks position is $0.611 \text{ nm} \pm 0.002$, that is 1.7% larger than for the crystallized 10 nm thin film.

In order to determine T_x , X-ray diffraction spectra for as-deposited clusters and thin films samples were recorded as a function of the temperature, with *in situ* annealing. The change in the thin film (220) diffraction peak from 150 °C to

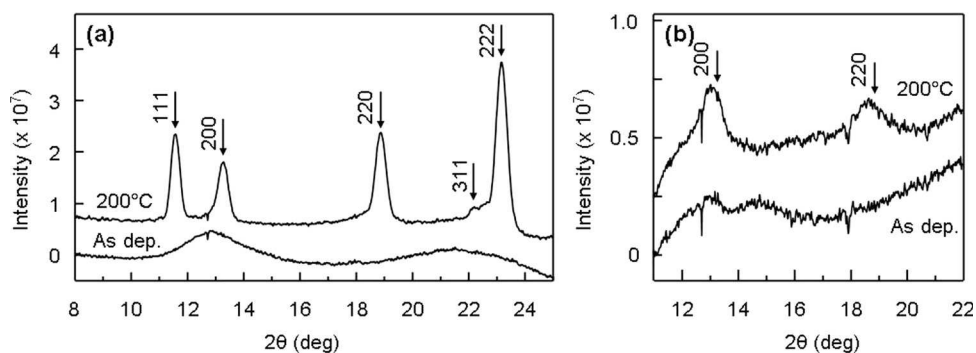


FIG. 1. X-ray diffraction spectra for (a) as-deposited and 200 °C *ex situ* annealed GST film and (b) clusters. Arrows in (a) and (b) indicate bulk GST fcc peaks position. Curves are shifted for clarity.

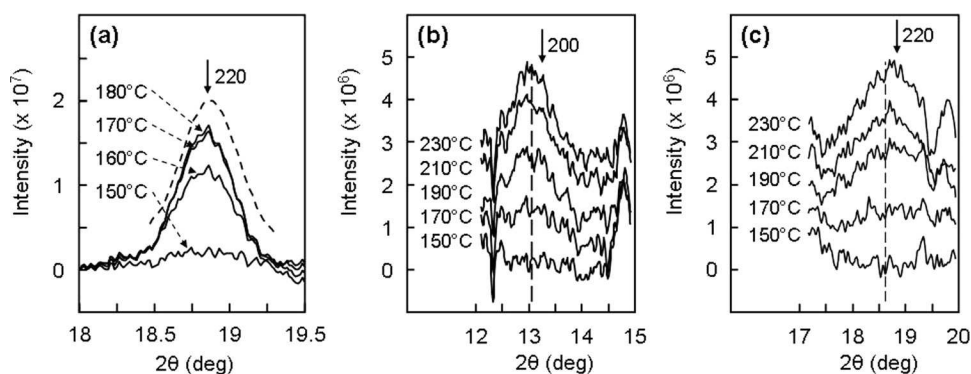


FIG. 2. (a) *In situ* annealed GST thin film (220) diffraction peak at different temperatures. Dotted line is the 200°C *ex situ* annealed thin film peak, measured at room temperature. Arrow indicates the bulk GST peak position. *In situ* annealed GST clusters (200) diffraction peak (b) and (220) diffraction peak (c) at different temperatures. In (b) and (c), curves are evenly shifted to ease viewing, arrows indicate the bulk GST peak position, and dotted lines indicate the 200°C *ex situ* annealed clusters peak positions, measured at room temperature.

180°C is plotted in Figure 2(a). Although the oven dome significantly decreases the signal to noise ratio, the peak intensity at 180°C is comparable with that of the *ex situ* annealed sample. At 150°C, no signal is recorded above background level, while at 170°C, the peak is close to its final amplitude. It can be observed that the (220) peak position at 180°C is slightly below that of the *ex situ* annealed thin film measured at room temperature, which can be explained by the GST thermal dilatation.¹⁹ The (200) and (220) diffraction peaks for *in situ* annealed clusters are shown in Figures 2(b) and 2(c). Despite the high noise level and spurious background contribution, the parallel rise in the amplitude for the two peaks is visible.

The crystallization temperature is obtained from the rise in the integrated intensity for the *in situ* annealed thin film and clusters (Figure 3) as the midpoint of the rise step. For the thin film, the rise is almost parallel for the (111) and the (220) peaks. T_x is equal to 155°C and the crystallization is almost completed at 160°C. For the clusters, T_x is close to 180°C and the rise in amplitude is more gradual, spanning from 150°C up to 200°C. It has to be observed that the crystallization temperature for the clusters is only 25°C above that of the 10 nm thin film. As already stated, there is no report of T_x values for GST nanoclusters of such small diameter in literature. One can try to compare our results with those reported in Ref. 3 on thin films of various thicknesses, embedded in Al₂O₃, which is the same cladding material as used in our work. Strikingly the crystallization temperature obtained for clusters (180°C) is much less than the value of 340°C reported in Ref. 3 for a thin film of 5 nm. Besides, T_x for our 10 nm thin film (155°C) is very close to the value

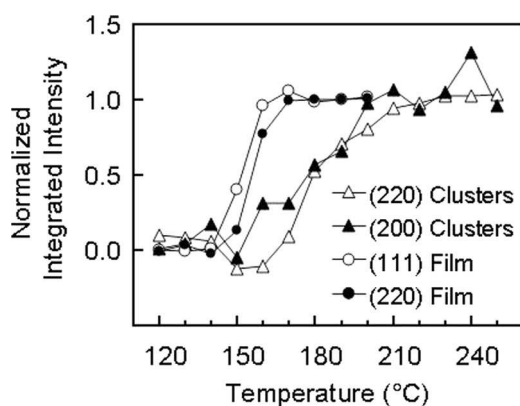


FIG. 3. Normalized integrated intensities for GST clusters (220) and (200), and GST film (111) and (220) diffraction peaks as a function of temperature.

reported in Ref. 3 for films with thickness above 10 nm, that is close to that of bulk GST.

The main result of the present work is the observation that even for nanoparticles with a diameter as small as 5 nm the phase change from the amorphous to the cubic state still takes place. Another important observation is that the out of plane lattice parameter for the crystalline fcc clusters is larger than that of the crystallized 10 nm thin film, the latter being very close to the lattice parameter measured in bulk fcc cubic GST. Besides, the film T_x is close to the bulk GST value. These two observations suggest a complete relaxation of strain in the 10 nm thin film cladded with Al₂O₃. The increase of the lattice parameter in clusters can be attributed to a large out of plane tensile strain due to the interaction with the oxide matrix. At the phase change, the bulk GST density decreases by 5%.¹⁸ While in thin films, the stress resulting from the volume change can be relaxed at crystallization by viscous flow in the amorphous phase,¹⁹ such a mechanism is less likely to take place in small particles embedded in an oxide matrix. The measured relative out of plane lattice parameter increase in clusters with respect to bulk GST value (1.7%) is close to one third of the volume relative change during the amorphous to crystalline phase change. This observation is in favor of an isotropic expansion of clusters and suggests that the volumes of the amorphous and crystalline clusters are similar due to the strong interaction with the embedding alumina, which is a far more rigid material than GST.

As already mentioned, the last important result is the small difference of T_x between clusters and thin films, in contrast with the strong thickness dependence of T_x reported in thin films cladded with Al₂O₃.³ However, it is hard to compare films and clusters since variations of T_x can result from many factors including different aspect ratio, intrinsic size effects, composition changes, matrix influence, and stress or strain effects. In our case, a possible composition effect could arise since, as compared with the films, the clusters are Te-depleted. For instance, the crystallization temperature in GST thin films with 10%–20% excess Sb is 15°C higher than for bulk films,²⁰ and the crystallization temperature for Ge₂Sb₂Te₄ is 175°C.²¹ In order to evaluate the consequences of the strain resulting from the phase change in clusters, it is instructive to evaluate the elastic energy stored in crystallized clusters since it will reduce the driving force for the phase transition. As a consequence, the kinetics for the phase change will be slowed, and during a temperature

scan, the transition temperature can be increased. In the case of GST, this driving force is 200 MJ/m^3 ,²² while an order of magnitude calculation for the elastic energy resulting from the strain is closer to 10 MJ/m^3 , which is not enough to induce significant effects.² Finally, intrinsic size effects could explain the increase of T_x observed in clusters.⁷

In conclusion, we grew nanometric GST clusters by a sputtering gas-aggregation technique, with narrow size distribution around 5.7 nm. Our results demonstrate the possibilities offered by this synthesis technique for the study of well calibrated, isolated or embedded clusters of phase change materials. Moreover, this method is close to other physical techniques used for PCM thin films deposition. The as-grown clusters dispersed in alumina are amorphous and transform into a cubic fcc crystalline phase at a well defined crystallization temperature of 180°C , which illustrates that the phase change in GST is also present in the sub-10 nm range. The crystalline clusters show a lattice parameter larger than that of bulk cubic GST, which indicates a tensile strain that is attributed to the interaction with the alumina matrix. Despite this significant interface coupling, the large increase in T_x observed in very thin GST films subjected to large interface stress is not seen in clusters. These results indicate that the scaling effect on the crystallization temperature in phase change material can be small, which is positive for their application in highly scaled PCRAM devices.

We thank J. F. Béar (Institut Néel) for his help during the ESRF experimental run and for the X-ray diffraction data analysis. Funding for this work was provided by the RTRA Fondation Nanoscience.

¹D. Lencer, M. Salinga, and M. Wuttig, *Adv. Mater.* **23**, 2030 (2011).

²R. E. Simpson, M. Krbal, P. Fons, A. V. Kolobov, J. Tominaga, T. Uruga, and H. Tanida, *Nano Lett.* **10**, 414 (2010).

- ³S. Raoux, J. Jordan-Sweet, and A. Kellock, *J. Appl. Phys.* **103**, 114310 (2008).
- ⁴H.-Y. Cheng, S. Raoux, and Y.-C. Chen, *J. Appl. Phys.* **107**, 074308 (2010).
- ⁵X. Wei, L. Shi, T. C. Chong, R. Zhao, and H. K. Lee, *Jpn. J. Appl. Phys., Part 1* **46**, 2211 (2007).
- ⁶S. Raoux, H.-Y. Cheng, J. L. Jordan-Sweet, B. Muñoz, and M. Hitzbleck, *Appl. Phys. Lett.* **94**, 183114 (2009).
- ⁷M. Zacharias and P. Streitenberger, *Phys. Rev. B* **62**, 8391 (2000).
- ⁸W. D. Nix, *Metall. Mater. Trans. A* **20**, 2217 (1989).
- ⁹S. Raoux, C. T. Rettner, J. L. Jordan-Sweet, A. J. Kellock, T. Topuria, P. M. Rice, and D. C. Miller, *J. Appl. Phys.* **102**, 094305 (2007).
- ¹⁰Y. Zhang, S. Raoux, D. Krebs, L. E. Krupp, T. Topuria, M. A. Caldwell, D. J. Milliron, A. Kellock, P. M. Rice, J. L. Jordan-Sweet, and H.-S. Philip Wong, *J. Appl. Phys.* **104**, 074312 (2008).
- ¹¹H. S. Choi, K. S. Seol, K. Takeuchi, J. Fujita, and Y. Ohki, *Jpn. J. Appl. Phys., Part 1* **44**, 7720 (2005).
- ¹²H. R. Yoon, W. Jo, E. H. Lee, J. H. Lee, M. Kim, K. Y. Lee, and Y. Khang, *J. Non-Cryst. Solids* **351**, 3430 (2005).
- ¹³G.-S. Park, J.-H. Kwon, M. Kima, H. R. Yoon, W. Jo, T. K. Kim, J.-M. Zuo, and Y. Khang, *J. Appl. Phys.* **102**, 013524 (2007).
- ¹⁴R. Morel, A. Brenac, P. Bayle-Guillemaud, C. Portemont, and F. La Rizza, *Eur. Phys. J. D* **24**, 287 (2003).
- ¹⁵H. R. Yoon, W. Jo, E. Cho, S. Yoon, and M. Kim, *J. Non-Cryst. Solids* **352**, 3757 (2006).
- ¹⁶S. Kohara, K. Kato, S. Kimura, H. Tanaka, T. Usuki, K. Suzuya, H. Tanaka, Y. Moritomo, T. Matsunaga, N. Yamada, Y. Tanaka, H. Suematsu, and M. Takata, *Appl. Phys. Lett.* **89**, 201910 (2006).
- ¹⁷In our experimental configuration (incident angle equal to 4° and integration of diffraction rings in a limited angular range), the measured diffracting planes are close to the sample plane. Hence the measured lattice parameter is close to, but not strictly equal to, the out of plane lattice parameter.
- ¹⁸T. Nonaka, G. Ohbayashi, Y. Toriumi, Y. Mori, and H. Hashimoto, *Thin Solid Films* **370**, 258 (2000).
- ¹⁹T. P. Leervad Pedersen, J. Kalb, W. K. Njoroge, D. Wamwangi, M. Wuttig, and F. Spaepen, *Appl. Phys. Lett.* **79**, 3597 (2001).
- ²⁰K. J. Choi, S. M. Yoon, N. Y. Lee, S. Y. Lee, Y. S. Park, B. G. Yu, and S. O. Ryu, *Thin Solid Films* **516**, 8810 (2008).
- ²¹M. Wuttig, D. Lüsebrink, D. Wamwangi, W. Welnic, M. Gillessen, and R. Dronskowski, *Nature Mater.* **6**, 122 (2007).
- ²²J. A. Kalb, M. Wuttig, and F. Spaepen, *J. Mater. Res.* **22**, 748 (2007).
- ²³See supplementary material at <http://dx.doi.org/10.1063/1.4769435> for the clusters size distribution and TEM images and the 2D images.